Phys Chem Minerals (2015) 42:431–439
DOI 10.1007/s00269-015-0734-0

ORIGINAL PAPER

Color mechanisms in spinel: cobalt and iron interplay for the blue color

Veronica D'Ippolito · Giovanni Battista Andreozzi · Ulf Hålenius · Henrik Skogby · Kathrin Hametner · Detlef Günther

Received: 4 November 2014 / Accepted: 13 January 2015 / Published online: 28 January 2015

Abstract Six natural, blue colored spinel crystals were studied chemically by electron microprobe and laser ablation inductively coupled plasma mass spectrometry (LA-ICP-MS) techniques and optically by UV–VIS–NIR–MIR spectroscopy in the range 30,000–2,000 cm^{-1} to investigate the causes of their blue color hues. The positions of the absorption bands vary only marginally with the principal composition of the samples (gahnite vs. spinel *s.s.*). Although blue colors in spinels are frequently the result of various electronic processes in Fe cations, we demonstrate by comparison with synthetic Co-bearing samples that Co acts as an important chromophore also in natural spinels. Already at concentration levels of a few ppm (e.g., >10 ppm), cobalt gives rise to absorption bands at ~18,000, 17,000 and 16,000 cm^{-1} that result in distinct blue coloration. In spinels with insignificant Co contents, different shades of paler blue (from purplish to greenish blue) colors are caused by electronic transitions in $^{T}Fe^{2+}$, $^{M}Fe^{2+}$, $^{M}Fe^{3+}$ and Fe^{2+}–Fe^{3+} cation pairs.

Keywords Spinel · Cobalt · Blue color · LA-ICP-MS · UV–VIS–NIR–MIR spectroscopy

V. D'Ippolito (✉) · G. B. Andreozzi
Dipartimento di Scienze della Terra, Sapienza Università di Roma, Piazzale Aldo Moro 5, 00185 Rome, Italy
e-mail: veronica.dippolito@uniroma1.it

U. Hålenius · H. Skogby
Department of Geosciences, Swedish Museum of Natural History, 10405 Stockholm, Sweden

K. Hametner · D. Günther
Laboratory of Inorganic Chemistry, Department of Chemistry and Applied Biosciences, ETH Zurich, Vladimir Prelog Weg 1, 8093 Zurich, Switzerland

Introduction

Due to their wide range of intense colors, high mechanical resistance and high thermal and chemical stability, minerals belonging to the spinel group are actively sought as gemstones, while synthetic spinel powders are widely used as ceramic pigment. The variability in color displayed by spinels is due to their ability to accommodate a wide range of transition metal cations of different valence states at their structural sites. The spinel structure (space group $Fd\bar{3}m$) consists of an approximately cubic close packed array of oxygen atoms, with cations found in tetrahedral (*T*) and octahedral (*M*) coordination. The *T* and *M* sites can be filled by A and B cations, where A are mainly divalent and B trivalent cations, respectively, resulting in AB_2O_4 stoichiometry. In general, spinels do not adhere to a configuration in which A cations occupy the *T* sites and B cations the *M* sites, but an octahedral—tetrahedral disorder of A and B cations may occur.

The degree of disorder is described by the so-called inversion parameter, *i*, which is defined as the fraction of trivalent B cations at the *T* sites, $^{T}(A_{1-i}B_i)^{M}(B_{2-i}A_i)_2O_4$. The inversion parameter can vary from zero, in the completely normal spinels, to one, in the completely inverse spinels, depending on composition, cation site preference, temperature and thermal history (Della Giusta et al. 1996; Princivalle et al. 1999; Andreozzi et al. 2000; Carbonin et al. 2002; Bosi et al. 2012).

Blue colored spinels have received considerable attention already from the early stages of human societies as gemstones, pigments for painting and ceramic pigments (Shigley and Stockton 1984; Llusar et al. 2001; Kock and de Waal 2007; Ahmed et al. 2009). Natural blue spinel gem is rather difficult to find in nature and the color can range from blue–gray to violet blue to greenish blue and

Table 1 The investigated natural blue spinel samples, their origin and color

Label	Nat.2	Nat.4	30070	440243	510942	800801
		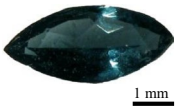		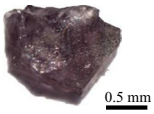		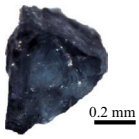
Color	Light blue	Greenish blue	Dark blue	Purplish blue	Blue	Blue
Origin	Tunduru, Tanzania	Tunduru, Tanzania	New Jersey, USA	Åker, Sweden	Levida, Spain	Catanzaro, Italy

vibrant blue. The characteristic intense color of the blue spinel made it possible to use them as highly priced sapphire analog in gemology. Blue pigment based on hercynite or cobalt-zinc aluminate spinel structure is widely used in ceramic industry (Llusar et al. 2001; Andreozzi et al. 2004; de Souza et al. 2009).

Blue natural and synthetic spinel crystals have been investigated by optical absorption spectroscopy in several studies (e.g., Gaffney 1973; Shigley and Stockton 1984; Schmetzer et al. 1989; Hålenius et al. 2002; Taran et al. 2005, 2009; Bosi et al. 2012; D'Ippolito et al. 2013; Fregola et al. 2014). In early studies, the blue color of natural spinels was attributed exclusively to the presence of Fe^{2+}, whereas cobalt was considered a coloring agent only in synthetic materials. Shigley and Stockton (1984) were the first authors to suggest that both cobalt and iron are capable of producing a blue color in natural gem materials. They collected absorption spectra of natural spinels containing up to 400 ppm Co and 2.7 wt% of Fe, and stated that both Fe and Co gave rise to absorption in the range 500–650 nm (20,000–15,380 cm^{-1}) without further analyses or assignments of the absorption bands superimposed in this spectral range. Later, Schmetzer et al. (1989) confirmed that low cobalt contents may contribute to the blue coloration in spinels. They investigated natural blue spinels with Co concentrations up to 60 ppm and Fe concentration up to 3.0 wt% and assigned tentatively the absorption spectra to superimposition of $^{T}Fe^{2+}$, $^{M}Fe^{2+}$, $^{M}Fe^{3+}$ and $^{T}Co^{2+}$ absorption bands.

Taran et al. (2009) recorded an optical absorption spectrum of a natural blue spinel from the island of Samos, which shows the highest cobalt concentrations among natural blue spinels optically investigated in literature. They speculated that the color of some natural blue spinels could be also due to the presence of minor amounts cobalt. Recently, Fregola et al. (2014) analyzed blue and green spinels and stated that an estimated concentration of 200 ppm of cobalt may have strongly influenced the blue color of their low Fe-bearing spinels. Nevertheless, the relative influence of cobalt *vs* iron on the coloration of natural blue spinels has not yet been evaluated in literature.

In order to explore the influence of Co on the blue color of natural spinels and thereby to test the hypothesis of Taran et al. (2009), comprehensive chemical analyses (major, minor and trace elements) together with optical absorption spectroscopy (UV–VIS–NIR–MIR) analyses were carried out on selected spinel crystals displaying different blue color hues.

Materials and methods

Six natural gem-quality, inclusion-free, single crystal of blue spinels originating from different geological environments around the world (Tanzania, Spain, Italy and USA) were studied. Four samples (30070, 440243, 510942 and 800801) belong to the mineral collection of the Swedish Museum of Natural History (Naturhistoriska rikmuseet, NRM) and two samples (Nat. 2, Nat. 4) were kindly made available by a private mineral collector. The crystals display colors ranging from purplish blue via light and dark blue to greenish blue. Color, specimen label and origin of the investigated spinels are reported in Table 1.

Electron microprobe (EMP) analysis

Electron microprobe analyses of the blue spinels were performed on natural single crystals mounted in polished and carbon-coated epoxy disks at CNR-IGAG lab c/o Sapienza University of Rome with a wavelength dispersive X-ray spectrometry (WDS) on a Cameca-Camebax SX50 instrument operating at an accelerating potential of 15 kV and a sample current of 15 nA, with an incident beam size of ~1 μm. No <5 spot analyses for each sample were performed to obtain average chemical compositions and estimates of the compositional homogeneity. Synthetic and natural standards used were corundum (Al), magnetite (Fe), wollastonite (Si), rutile (Ti), vanadinite (V), metallic Zn, Mn, Co and Ni and synthetic $MgAl_2O_4$ (Mg) and $MgCr_2O_4$ (Cr) spinel single crystals characterized by Andreozzi et al. (2000) and Hålenius et al. (2010), respectively. A PAP CAMECA program was used to convert X-ray counts into weight percentages of the corresponding oxides.

Laser ablation inductively coupled plasma mass spectrometry (LA-ICP-MS)

Major, minor and trace element composition of the blue spinels was determined by LA-ICP-MS analyses. The analyses were carried out using an 193 nm ArF excimer laser ablation system (Lambda Physik, Göttingen Germany) with an energy of 22 J/cm^2, coupled to an ICP-MS (DRC II +, Perkin Elmer, Norwalk, USA) (Ottinger et al. 2005). The samples were ablated for 40 s (10 Hz, 60 µm crater diameter). Regarding the instrumental settings, the He carrier, nebulizer, auxiliary and coolant gas flow rates were 1.2, 0.85, 0.75 and 17.5 L min^{-1}, respectively, with a RF power of 1,380 W. Regarding the data acquisition parameters, the dwell time was 10 ms with a dual (pulse and analog counting) detector mode. For all measurements, the samples were placed inside the ablation cell with the reference material NIST SRM 610 used as external calibration standard, while Al was used as internal standard. Data reduction and concentration calculation were carried out using the protocol as described in Longerich et al. (1996) on the isotopes ^{7}Li, ^{9}Be, ^{11}B, ^{23}Na, ^{25}Mg, ^{27}Al, ^{29}Si, ^{39}K, ^{42}Ca, ^{49}Ti, ^{51}V, ^{53}Cr, ^{55}Mn, ^{57}Fe, ^{59}Co, ^{60}Ni, ^{65}Cu, ^{66}Zn and ^{71}Ga.

Optical absorption spectroscopy and Fourier transform infrared (UV–VIS–NIR–MIR) spectroscopy

Unpolarized room-temperature optical absorption spectra were recorded on the blue single crystals in the spectral range 270–1,100 nm (37,037–9,091 cm^{-1}) at a spectral resolution of 1 nm using an AVASPEC-ULS2048X16 spectrometer attached via a 400 µm UV optical fiber to a Zeiss Axiotron UV-microscope. The crystals analyzed by optical absorption spectroscopy are the same as the ones used for the EMP analyses. These crystals were embedded in a thermoplastic resin, placed on a glass slide and polished on two parallel surfaces. The resulting thickness of each absorber was in the range 0.11–2.36 mm as determined by means of a digital micrometer. A 75 W Xenon arc lamp served as illuminating source and a photomultiplier as detector. Spectra in the NIR spectral region from 1,100 to 2,000 nm (9,091–5,000 cm^{-1}) were recorded on the same crystals with a Zeiss MPM800 single beam

Table 2 Chemical composition of the investigated natural blue spinel samples (EMP data in wt%)

Sample	Nat. 2	Nat. 4	30070	440243	510942	800801
SiO2	0.02(1)	0.01(2)	0.15(4)	0.02(1)	0.01(1)	0.05(3)
TiO2	0.00	0.01(1)	0.03(4)	0.03(3)	0.00	0.00
Al_2Oa	70.14(81)	70.52(57)	53.91(15)	70.21(45)	56.62(19)	68.49(84)
V2O3	0.01(1)	0.08(2)	0.02(2)	0.02(2)	0.01(1)	0.00
O2O3	0.01(2)	0.02(1)	0.03(4)	0.02(1)	0.01(1)	0.02(3)
FeOtot	1.83(9)	1.47(3)	1.82(1)	2.52(5)	6.71(48)	3.15(13)
MgO	27.18(25)	27.76(29)	0.08(3)	26.66(25)	1.49(6)	23.41(25)
ZnO	0.21(6)	0.13(9)	42.97(1.3)	0.51(11)	36.32(57)	5.17(34)
MnO	0.04(4)	0.01(2)	0.02(2)	0.14(5)	0.19(5)	0.43(5)
CoO	0.03(3)	0.01(1)	0.01(2)	0.01(1)	0.03(1)	0.07(2)
NiO	0.01(2)	0.01(2)	0.00	0.01(1)	0.02(3)	0.03(3)
Total	99.50	100.03	99.04	100.15	101.41	100.82
Cations on the basis of 4 oxygens						
Si	0.000	0.000	0.005(2)	0.000	0.000	0.001(1)
Ti	0.000	0.000	0.001(1)	0.001(1)	0.000	0.000
Al	1.985(2)	1.984(8)	1.962(14)	1.983(4)	1.970(3)	1.976(7)
V	0.000	0.001(1)	0.001(1)	0.000	0.000	0.000
Cr	0.000	0.000	0.001(1)	0.000	0.000	0.000
Fe^3+	0.014(2)	0.015(1)	0.026(1)	0.015(1)	0.029(5)	0.022(3)
Fe^{2+}	0.023(2)	0.014(1)	0.021(2)	0.036(1)	0.137(6)	0.043(3)
Mg	0.972(2)	0.984(12)	0.004(1)	0.953(6)	0.066(3)	0.854(6)
Zn	0.004(1)	0.002(2)	0.980(14)	0.009(2)	0.792(13)	0.094(7)
Mn	0.001(1)	0.000	0.001(1)	0.003(1)	0.005(1)	0.008(1)
Co	0.001(1)	0.000	0.000	0.000	0.001(1)	0.002(1)
Ni	0.000	0.000	0.000	0.000	0.000	0.000
Total	3.000	3.000	3.000	3.000	3.000	3.000

Fe^{2+} and Fe^{3+} contents from charge balance. Experimental standard deviation in brackets

Table 3 Major, minor and trace element contents of the investigated natural blue spinel samples (LA-ICP-MS and EMP data in ppm)

Sample	Nat. 2		Nat. 4		30070		440243		510942		800801	
	LA-ICP-MS	EMP	LA-ICP-MS	EMP	LA-ICP-MS	EMP	LA-ICP-MS	EMP	LA-ICP-MS	EMP	LA-ICP-MS	EMP
Al	372,800	372,848	371,200	371,203	285,300	285,327	371,600	371,610	299,700	269,672	362,500	362,485
Mg	163,560	164,017	171,960	168,111	860	494	171,700	160,792	8,170	8,990	135,400	141,157
Zn	1,130	1,652	310	516	370,380	345,250	4,650	4,083	380,200	291,789	53,780	41,529
Fe	13,060	14,811	10,700	12,276	12,650	14,108	18,840	19,602	47,520	52,175	22,680	24,485
Mn	140	187	60	60	168	108	1,160	1,117	1,308	1,497	2,750	3,334
V	5.1	116	162	252	77	150	52	139	227	95	3.8	25
Cr	4.1	98	322	604	4.8	174	21	138	4.5	67	2.8	115
Si	337	61	242	165	902	715	418	74	264	33	648	228
Co	13.3	31	14	132	1.4	118	7.7	67	107	260	611	514
Ga	136	–	151	–	67	–	150	–	178	–	209	–
Ti	4.80	22	71	85	48	171	71	85	11	27	2.5	6
Ni	23.4	130	40	255	3.1	0	40	255	30	145	80	195
Cu	0.72	–	1.2	–	3.4	–	1	–	2.2	–	3.5	–
Li	47.5	–	10.4	–	0.72	–	5.8	–	9.9	–	32	–
Be	12.9	–	3.0	–	1.1	–	7.5	–	2.3	–	1.6	–
B	5.1	–	4.2	–	2.7	–	3.3	–	3.6	–	5.5	–
Na	0.40	–	–	–	5.4	–	0.7	–	2.5	–	2.8	–
K	–	–	5.3	–	16	–	–	–	4.7	–	5.1	–
Ca	73	–	–	–	1,480	–	78	–	464	–	718	–

microscope-spectrometer using a 100 W halogen lamp as light source and concave gratings as monochromator. Light detection was achieved by means of a photoconductive PbS-cell. The NIR spectra were recorded at a spectral resolution of 5 nm. Zeiss Ultrafluar 10× lenses served as objective and condenser in all measurements. The size of the circular measure aperture ranged from 40 to 64 µm in diameter. The wavelength scale of the spectrometers was calibrated against Ho_2O_3-doped and Pr_2O_3/Nd_2O_3-doped standards (Hellma glass filters 666F1 and 666F7) with accuracy better than 15 cm^{-1}.

Spectroscopic data were also collected within the NIR–MIR range by means of a FTIR spectrometer (Bruker Equinox 55) equipped with a tungsten lamp source and a CaF_2 beamsplitter. Most samples were measured in the 2,000–13,000 cm^{-1} range using a InSb detector, but two samples (#510942, #800801) were measured in the 2,000–12,000 cm^{-1} range via an IR microscope equipped with an MCT detector. Spectra were collected on the same single crystals as above but with a thickness in the range 70–429 µm during 128 or 256 cycles at a spectral resolution of 8 cm^{-1}. The sizes of the measure apertures ranged from 50 to 300 µm.

Recorded spectra in the UV–VIS–NIR–MIR range were deconvoluted using the peak resolution program Jandel PeakFit 4.12. In the deconvolution process, all fitted bands were assumed to be of Gaussian shape. The recorded UV-absorption edges were also fitted with a Gaussian function. No other constraints were applied during the fitting procedure.

Results and discussion

Chemical data

Chemical analyses of major elements obtained by EMP (Table 2) and major, minor and trace elements obtained by LA-ICP-MS (Table 3) were measured on the same respective crystal. The investigated spinels contain Al as major trivalent cation and Mg or Zn as major divalent cations. Four crystals (Nat. 2, Nat. 4, 440243 and 800801) show a prevalent spinel *s.s.* ($MgAl_2O_4$) end-member component, and the two remaining crystals (30070 and 510942) show a prevalent gahnite ($ZnAl_2O_4$) end-member component. The remaining component of all samples (2–20 %) is dominated by Fe, primarily Fe^{2+}. The amount of Fe^{2+} and Fe^{3+} were calculated on the basis of charge balance requirements and the spinel stoichiometry (three cations per four anions). Furthermore, minor contents of Mn, up to 0.008 apfu and Co up to 0.002 apfu, were measured in some samples.

Results of the two different analytical approaches are reported in terms of parts per million (ppm) in Table 3. A

Table 4 Chemical formulae of the investigated natural blue spinel samples (in apfu). The dominant component at the respective cation site is written in bold

apfu atoms per formula unit. Fe^{2+} and Fe^{3+} contents from charge balance

Nat. 2	$(\mathbf{Mg}_{0.974}Zn_{0.003}Fe^{2+}_{0.025})_{\Sigma1.002}(\mathbf{Al}_{1.988}Fe^{3+}_{0.008}Si_{0.002})_{\Sigma1.998}O_4$
Nat. 4	$(\mathbf{Mg}_{0.985}Zn_{0.001}Fe^{2+}_{0.016})_{\Sigma1.002}(\mathbf{Al}_{1.984}Fe^{3+}_{0.012}Cr_{0.001}Si_{0.001})_{\Sigma1.998}O_4$
30070	$(Mg_{0.007}\mathbf{Zn}_{0.981}Fe^{2+}_{0.018})_{\Sigma1.006}(\mathbf{Al}_{1.964}Fe^{3+}_{0.024}Si_{0.006})_{\Sigma1.994}O_4$
440243	$(\mathbf{Mg}_{0.952}Zn_{0.010}Fe^{2+}_{0.037}Mn_{0.003})_{\Sigma1.002}(\mathbf{Al}_{1.983}Fe^{3+}_{0.012}Si_{0.002}Ti_{0.001})_{\Sigma1.998}O_4$
510942	$(Mg_{0.060}\mathbf{Zn}_{0.797}Fe^{2+}_{0.140}Mn_{0.004})_{\Sigma1.001}(\mathbf{Al}_{1.984}Fe^{3+}_{0.012}Si_{0.002}V_{0.001})_{\Sigma1.999}O_4$
800801	$(\mathbf{Mg}_{0.856}Zn_{0.094}Fe^{2+}_{0.045}Mn_{0.007}Co_{0.002})_{\Sigma1.004}(\mathbf{Al}_{1.979}Fe^{3+}_{0.014}Si_{0.003})_{\Sigma1.996}O_4$

good agreement between the two datasets is observed with exception of the elements close to the detection limit of the EMP (ca. 300 ppm), for which obviously LA-ICP-MS is generally more reliable. Thus, to obtain the best chemical characterization of each sample, major elements (Mg, Zn and Al) were selected from EMP results, and minor and trace elements were selected from LA-ICP-MS results. The resulting chemical formulae are reported in atoms per formula unit (apfu) in Table 4.

NIR–MIR spectra

All the natural blue spinels show an intense absorption band in the NIR range centered at ~5,000 cm^{-1} (Fig. 1) that has been widely attributed to the spin-allowed electronic *d–d* transition ($^5E \rightarrow {}^5T_2$) in tetrahedrally coordinated Fe^{2+} (Rossman and Taran 2001; Taran and Langer 2001; Skogby and Hålenius 2003; Lenaz et al. 2004; Taran et al. 2005; Hofmeister 2007). The band is characterized by a distinct shoulder at ~3,500 cm^{-1}, due to the dynamic Jahn–Teller effect of $^TFe^{2+}$ in the spinel structure (Skogby and Hålenius 2003; Taran et al. 2005). The best fit of the $^TFe^{2+}$ absorption envelope in the range 2,000–9,000 cm^{-1} was obtained by applying the four-band model proposed by Skogby and Hålenius (2003). The parameters obtained through curve fitting are summarized in Table 5. Skogby and Hålenius (2003) showed an excellent linear correlation between integral absorption coefficient (A_{SUM}) of the split $^5E \rightarrow {}^5T_2$ and the $^TFe^{2+}$ concentration. The Fe^{2+} contents derived from the optical absorption spectra are in reasonable agreement with those calculated from the EMP analyses under charge balance consideration, with some discrepancy probably due to approximation of the charge balance method and possible vertical chemical zoning of the sample.

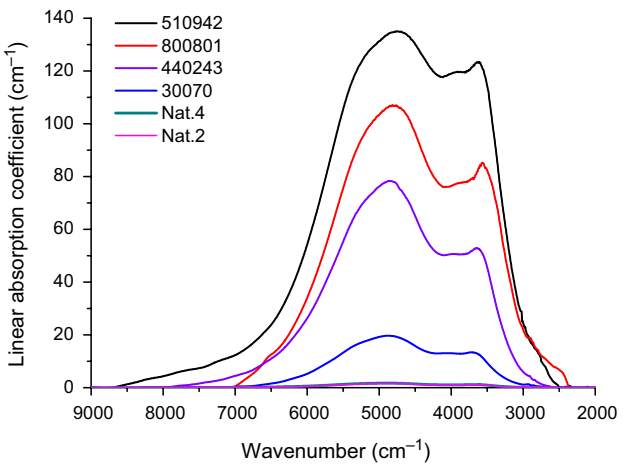

Fig. 1 Net NIR–MIR absorption spectra of the investigated natural blue spinels. The spectra of the samples Nat. 2 and Nat. 4 overlap

UV–VIS–NIR spectra

Optical absorption spectra of all the present samples are shown in Fig. 2. Excepting band intensities and the detailed band structure in the range 15,000–22,000 cm^{-1}, the absorption spectra show strong similarities, and they are characterized by a series of absorption bands with low to intermediate intensity superimposed on an intense UV edge. For all the present spectra, at least ten Gaussian curves were necessary for satisfactory fits. For the sake of simplicity, a common labeling from *a* to *m* was used for the fitted bands in the spectra of the blue colored spinels (Fig. 3; Table 6). The positions of the absorption bands vary only marginally with the principal composition of the samples (gahnite vs. spinel *s.s.*), but the band intensities are strongly influenced by differences in total iron content, iron valency distribution and Fe cation site distribution (Tables 2, 3, 4). In spectra of blue colored spinels with high Fe contents and comparatively insignificant Co contents, one observes a large set of absorption bands in the spectral region between 10,000 and 20,000 cm^{-1}. In accordance with previous assignments (e.g., Schmetzer et al. 1989; Hålenius et al. 2002; Taran et al. 2005; D'Ippolito et al. 2013; Fregola et al. 2014), we have assigned these bands to spin-forbidden electronic transitions in $^TFe^{2+}$, $^MFe^{2+}$, $^MFe^{3+}$ as well as Fe^{2+}–Fe^{3+} intervalence charge transfer transitions and Fe^{2+}–Fe^{3+} exchange coupled pair transitions (Table 6). The relative intensity of these Fe-related absorption bands determines the shade of the blue color of the individual spinels. Spinels with iron exclusively or dominantly present as $^TFe^{2+}$ show a purplish blue tinge (as sample 440243), whereas spectra of spinels with increasing contents of $^MFe^{3+}$ show increasing intensities of the absorption at 17,000 cm^{-1} (*g*) that result in purer blue color

Table 5 Results of the curve fitting of split $^5E \rightarrow {}^5T_2$ band due to $^TFe^{2+}$ in NIR and MIR spectra of the investigated natural blue spinel samples

	Nat. 2	Nat. 4	30070	440243	510942	800801
Thickness (μm)	279	429	245	157	70	126
ν_1	4,973	4,989	4,949	4,953	5,123	5,080
α_1	1.49	1.65	18.8	82.39	127.15	97.98
ω_1	1,550	1,495	1,426	1,717	1,632	1,561
A_1	2,459	2,630	28,550	150,620	220,910	162,750
ν_2	4,617	4,564	4,641	4,660	4,445	4,485
α_2	0.14	0.20	1.49	4.84	40.91	25.09
ω_2	597	658	481	2,930	708	809
A_2	89	138	764	568	308,500	21,616
ν_3	4,081	4,022	4,067	4,082	4,086	4,002
α_3	0.23	0.40	4.89	7.73	26.117	29.07
ω_3	401	426	438	349	416	436
A_3	97	180	2,281	2,873	11,556	13,482
ν_4	3,624	3,610	3,651	3,618	3,635	3,579
α_4	0.86	0.93	10.61	44.66	106.12	66.37
ω_4	622	522	504	649	678	541
A4	573	518	5,694	30,840	76,610	38,250
A_{sum}	3,218	3,466	37,289	187,264	339,926	236,097

ν wavenumber (cm^{-1}); α linear absorption coefficient (cm^{-1}); ω full width at half maximum; A integral absorption coefficient (cm^{-2})

hues (as sample 30070). With a concomitant increase of $^MFe^{2+}$ and $^MFe^{3+}$ contents, as in sample Nat. 4, an absorption band (*i*) at ~15,000 cm^{-1} becomes a prominent spectral feature that causes a distinct greenish tinge in blue spinels. Hence, small variations in total iron content, Fe cation valency distribution and site distribution determine the color hue of the spinel.

Spectra of some of the investigated blue colored spinel samples (Nat. 2, Nat. 4, 510942 and 800801) show an additional absorption band at ~16,000 cm^{-1} (band *h* in Table 6). The chemical analyses of these specimens reveal enhanced Co contents from 13 to 611 ppm. Cobalt concentrations at these levels may be sufficient to influence the color and consequently also the absorption spectra of spinels, as hypothesized previously (Shigley and Stockton 1984; Schmetzer et al. 1989; Taran et al. 2009; Fregola et al. 2014). At closer inspection, it is evident that the spectra of these samples show distinct absorption bands in the VIS range at ~18,000, ~17,000 and ~16,000 cm^{-1} (labeled

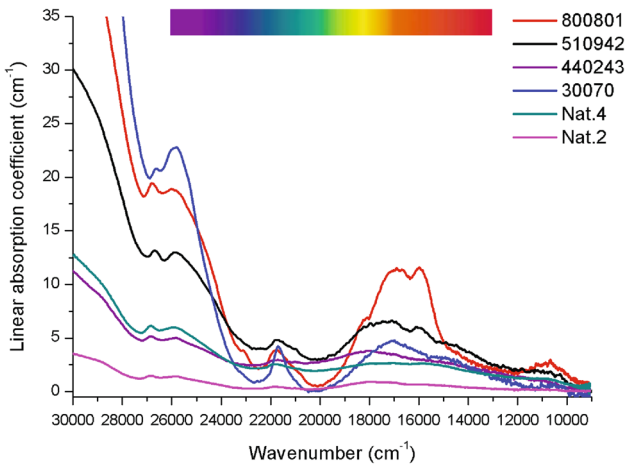

Fig. 2 Optical absorption spectra of the investigated natural blue spinels in the UV–VIS–NIR range

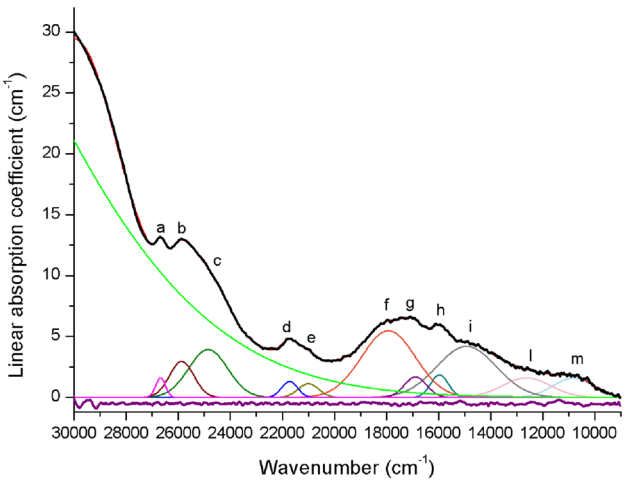

Fig. 3 The curve resolved UV–VIS–NIR spectrum spinel sample 510942. The *thick black line* represents experimental data, the *red line* (*overlapped to the black one*) represents the sum of the fitted Gaussian shaped bands, the *violet line* (*at the bottom of the figure*) represents the difference between the observed and the calculated spectra

Table 6 Results of the curve fitting of the UV–VIS–NIR spectra of the investigated natural blue spinel samples

	Nat. 2			Nat. 4			30070			440243			510942			800801			Assignment
	ν	α	ω	ν	α	ω	ν	α	ω	ν	α	ω	ν	α	ω	ν	α	ω	
a	26,825	0.36	194	26,840	0.78	385	26,640	9.30	415	26,794	1.18	300	26,676	1.61	241	26,850	2.70	315	s.f. $^{5}E \rightarrow {}^{3}E$ of $^{T}Fe^{2+}$
b	25,956	0.51	438	25,950	1.16	543	25,730	13.38	433	25,910	1.62	456	25,863	2.53	446	25,989	12.35	979	s.f. $^{5}E \rightarrow {}^{3}T_2$, $^{3}T_1$ of $^{T}Fe^{2+}$
c	24,852	0.44	731	24,675	2.21	1925	24,870	7.53	621	24,854	1.85	712	24,850	3.43	741	24,740	7.54	1,073	s.f. $^{6}A_{1g} \rightarrow {}^{4}E_g$ (^{4}D) of $^{M}Fe^{3+}$
d	21,775	0.27	398	21,737	0.81	516	21,656	3.33	233	21,820	0.84	472	21,715	1.30	303	21,826	2.82	385	s.f. $^{6}A_{1g} \rightarrow {}^{4}A_{1g}$, $^{4}E_g$ transition of $^{M}Fe^{3+}$
e	20,955	0.11	154	20,883	0.13	324	21,112	0.48	258	20,994	0.92	739	20,996	1.13	340	21,120	1.69	498	
f	17,986	0.61	728	17,980	1.61	821	17,943	1.68	855	18,049	3.55	1,977	18,300	3.99	669	18,314	3.33	406	s.f. $^{5}E \rightarrow {}^{3}T_2$ of $^{T}Fe^{2+}$ s.a. $^{4}A_2(F) \rightarrow {}^{4}T_1(P)$ of $^{T}Co^{2+}$
g	17,004	0.53	573	17,059	0.86	688	16,932	3.38	950	16,988	0.08	95	17,035	3.45	669	17,021	10.68	748	s.f. $^{5}E \rightarrow {}^{3}T_1$ of $^{T}Fe^{2+}$ s.a. $^{4}A_2(F) \rightarrow {}^{4}T_1(P)$ of $^{T}Co^{2+}$
h	15,843	0.29	440	15,911	0.60	554	–	–	–	–	–	–	15,850	1.44	396	15,816	5.55	379	s.a. $^{4}A_2(F) \rightarrow {}^{4}T_1(P)$ of $^{T}Co^{2+}$
i	14,906	0.42	1,481	14,854	1.92	1,395	14,842	2.22	752	14,944	1.50	1,140	14,814	3.98	1,696	14,945	3.84	1,166	$^{M}Fe^{2+} \leftrightarrow {}^{M}Fe^{3+}$ IVCT $^{T}Fe^{2+} \leftrightarrow {}^{M}Fe^{3+}$ ECP
l	12,748	0.09	2,365	12,604	0.38	788	12,627	0.71	898	12,728	1.33	1,081	12,617	0.39	684	12,778	1.10	600	s.f. $^{5}E \rightarrow {}^{3}T_1$ of $^{T}Fe^{2+}$ $^{T}Fe^{2+} \leftrightarrow {}^{M}Fe^{3+}$ ECP
m	10,904	0.14	978	10,905	1.05	1,080	10,629	0.56	345	10,939	0.64	788	10,828	1.58	807	10,848	2.56	908	s.a. $^{5}T_{2g} \rightarrow {}^{5}E_g$ in $^{M}Fe^{2+}$

ν wavenumber (cm^{-1}); α linear absorption coefficient (cm^{-1}); ω full width at half maximum. *s.f.* spin-forbidden, *s.a.* spin-allowed, *IVCT* intervalence charge transfer, *ECP* exchange coupled pair. The assignment of absorption bands to different transitions was made in agreement with previous studies (Schmetzer et al. 1989; Hålenius et al. 2002; Taran et al. 2005; D'Ippolito et al. 2013; Fregola et al. 2014)

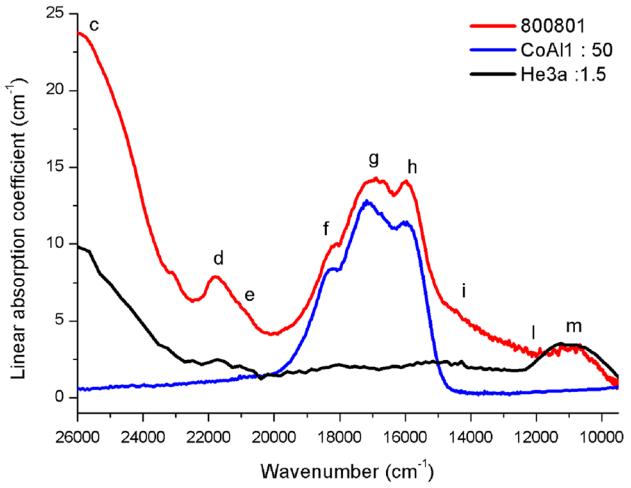

Fig. 4 Optical absorption spectrum of the sample 800801 compared to calculated spectra using spectral data of a synthetic Co-bearing spinel (sample CoAl10 in Bosi et al. 2012) and Fe-bearing spinel (sample He3a in Hålenius et al. 2002). The spectra of the synthetic spinels were divided by scaling factors (based on chemical compositions: 50 and 1.5, respectively) to simulate the spectrum of the sample 800801

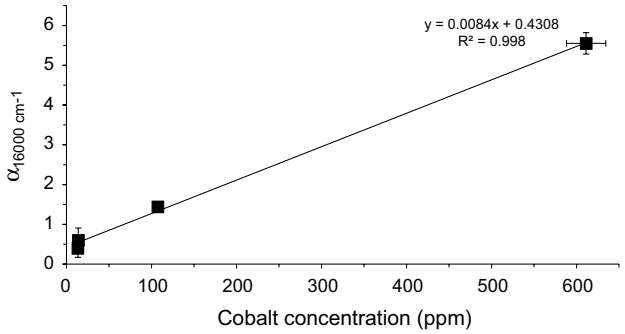

Fig. 5 Relationship between the linear absorption coefficient of the absorption band at ~16000 cm^{-1} and the Co content (in ppm) in our Co-bearing samples. *Error bars* are indicated. When they do not appear, the errors are equal or minor the symbol

f, g, h). The latter of these bands is masked by the relatively weak Fe-related bands at ~18,000 and ~17,000 cm^{-1} in spectra of the blue spinels with Co contents below 10 ppm. It is noteworthy that optical absorption spectra of synthetic single crystals belonging to the $(Mg,Co)Al_2O_4$ series show strong absorption bands due to spin-allowed $^4A_2$ (F) → $^4T_1$(P) transitions in $^TCo^{2+}$ at ~18,000, ~17,000 and ~16,000 cm^{-1} (Bosi et al. 2012).

In order to explore the role of cobalt as a color agent in the present samples, we compared the spectrum of sample 800801 with optical absorption spectra scaled to the same Fe and Co contents (Fig. 4) using data from the optical absorption spectra of synthetic Co- and Fe-bearing spinels (Bosi et al. 2012; Hålenius et al. 2002). It is evident from this comparison that iron is not responsible for the color determining absorption bands (*f*, *g* and *h*) in the visible spectral range of sample 800801. On the contrary, it demonstrates that cobalt, already at low concentration levels (~600 ppm corresponding to 0.002 apfu), strongly influences the color of natural blue spinels by very intense absorption bands caused by spin-allowed $^4A_2$ (F) → $^4T_1$(P) electronic *d–d* transitions in Co^{2+} at ~18,000, 17,000 and 16,000 cm^{-1}. The observed high intensities of these absorption bands reflects the fact that spin-allowed *d–d* bands caused by tetrahedrally coordinated Co^{2+} display the highest oscillator strengths of all 3*d* cation-related absorption bands and may be detected in optical absorption spectra even at $^TCo^{2+}$ concentrations as low as 1 ppm (Marfunin 1979). The linear absorption coefficients recorded for the band at ~16,000 cm^{-1} in our samples Nat. 2, Nat. 4, 510942 and 800801 are in good agreement (Fig. 5) with the experimental data for synthetic $(Co,Mg)Al_2O_4$ solid solution crystals (Bosi et al. 2012). It is instructive that even in the spectra of samples Nat. 2 and Nat. 4, that have Co concentrations of only ~13 ppm, a small but significant absorption band is observed at 16,000 cm^{-1}.

Conclusions

The color of natural spinels is enhanced by the presence of Co, even at very low concentrations (e.g., >10 ppm). Tetrahedrally coordinated Co^{2+} gives rise to a strong and diagnostic absorption band at ~16,000 cm^{-1} as well as absorption bands at ~18,000 and 17,000 cm^{-1} that overlap bands caused by electronic transitions in Fe cations. In particular, when iron and cobalt are present in comparable amounts, the electronic transitions in cobalt have much stronger influence on the spinel color than those related to iron, thus producing more intense blue colors.

When Co contents are extremely low to insignificant (e.g., <10 ppm), the different shades of paler blue colors observed in spinels are related to the total iron content as well as the valency and site distribution of iron over the *T* and *M* sites. It is proved here that the Fe-related absorption bands are caused by electronic transitions in $^TFe^{2+}$, $^MFe^{2+}$, $^MFe^{3+}$ and Fe^{2+}–Fe^{3+} cation pairs: Purplish blue colors occur in spinels when $^TFe^{2+}$ is the dominating iron species; purer blue colors are observed in spinels with increasing $^TFe^{2+}$ and $^MFe^{3+}$ contents, whereas the blue color takes on a distinct greenish tinge in spinels when Fe^{2+}–Fe^{3+} transitions occur.

Acknowledgments The present study benefited from financial support from the Synthesys European Programme at NRM (Swedish Museum of Natural History, Stockholm) and "Progetto Sapienza Avvio alla Ricerca 2012". P. Patriarca is thanked for kindly providing the samples Nat. 2 and Nat. 4. The assistance of M. Serracino during EMP data collection is gratefully acknowledged. Comments

and suggestions by Michail N. Taran and Remo Widmer are highly appreciated.

References

Ahmed IS, Shama SA, Moustafa MM, Dessouki HA, Ali AA (2009) Synthesis and spectral characterization of $Co_xMg_{1-x}Al_2O_4$ as new nano-coloring agent of ceramic pigment Spectrochim Acta A 74:665–672. doi:10.1016/j.saa

Andreozzi GB, Princivalle F, Skogby H, Della Giusta A (2000) Cation ordering and structural variations with temperature in $MgAl_2O_4$ spinel: an X-ray single-crystal study. Am Miner 85:1164–1171

Andreozzi GB, Hålenius U, Skogby H (2001) Spectroscopic active $^{IV}Fe^{3+}$–$^{VI}Fe^{3+}$ clusters in spinel-magnesioferrite solid solution crystals: a potential monitor for ordering in oxide spinels. Phys Chem Miner 28:435–444. doi:10.1007/s002690100178

Andreozzi GB, Baldi G, Bernardini GP, Di Benedetto F, Romanelli M (2004) ^{57}Fe Mössbauer and electronic spectroscopy study on a new synthetic hercynite-based pigment. J Eur Ceram Soc 24:821–824. doi:10.1016/S0955-2219(03)00329-7

Bosi F, Hålenius U, D'Ippolito V, Andreozzi GB (2012) Blue spinel crystals in the $MgAl_2O_4$–$CoAl_2O_4$ series: part II. Cation ordering over short-range and long-range scales. Am Miner 97:1834–1840. doi:10.2138/am.2012.4139

Carbonin S, Martignago F, Menegazzo G, Dal Negro A (2002) X-ray single-crystal study of spinels: in situ heating. Phys Chem Miner 29:503–514. doi:10.1007/s00269-002-0262-6

de Souza LKC et al. (2009) Blue pigments based on $Co_xZn_{1-x}Al_2O_4$ spinels synthesized by the polymeric precursor method. Dyes Pigments 81:187–192. doi:10.1016/j.dyepig.2008.09.017

Della Giusta A, Carbonin S, Ottonello G (1996) Temperature-dependent disorder in a natural Mg–Al–Fe^{2+}–Fe^{3+} spinel. Miner Mag 60:603–616

D'Ippolito V, Andreozzi GB, Bosi F, Hålenius U, Mantovani L, Bersani D, Fregola RA (2013) Crystallographic and spectroscopic characterization of a natural Zn-rich spinel approaching the end-member gahnite ($ZnAl_2O_4$) composition. Miner Mag 77:2941–2953. doi:10.1180/minmag.2013.077.7.05

Fregola RA, Skogby H, Bosi F, D'Ippolito V, Andreozzi GB, Hålenius U (2014) Optical absorption spectroscopy study of the causes for color variations in natural Fe-bearing gahnite: insights from iron valency and site distribution data. Am Miner 99:2187–2195. doi:10.2138/am-2014-4962

Gaffney ES (1973) Spectra of Tetrahedral Fe^{2+} in $MgAl_2O_4$. Phys Rev B 8:3484–3486. doi:10.1103/PhysRevB.8.3484

Hålenius U, Skogby H, Andreozzi GB (2002) Influence of cation distribution on the optical absorption spectra of Fe3 + -bearing spinel *s.s.*-hercynite crystals: evidence for electron transitions in $^{VI}Fe2^{+}$–$^{VI}Fe3^{+}$ clusters. Phys Chem Miner 29:319–330. doi:10.1007/s00269-002-0240-z

Hålenius U, Andreozzi GB, Skogby H (2010) Structural relaxation around Cr^{3+} and the red-green color change in the spinel (sensu stricto)-magnesiochromite ($MgAl_2O_4$–$MgCr_2O_4$) and gahnite-zincochromite ($ZnAl_2O_4$–$ZnCr_2O_4$) solid-solution series. Am Miner 95:456–462. doi:10.2138/am.2010.3388

Hofmeister AM (2007) Thermal diffusivity of aluminous spinels and magnetite at elevated temperature with implications for heat transport in Earth's transition zone. Am Miner 92:1899–1911. doi:10.2138/am.2007.2589

Kock LD, De Waal D (2007) Raman studies of the underglaze blue pigment on ceramic artefacts of the Ming dynasty and of unknown origins. J Raman Spectrosc 38:1480–1487. doi:10.1002/jrs.1805

Lenaz D, Skogby H, Princivalle F, Hålenius U (2004) Structural changes and valence states in the $MgCr_2O_4$–$FeCr_2O_4$ solid solution series. Phys Chem Miner 31:633–642. doi:10.1007/s00269-004-0420-0

Llusar M, Forés A, Badenes JA, Calbo J, Tena MA, Monrós G (2001) Colour analysis of some colbat-based blue pigments. J Eur Ceram Soc 21:1121–1130. doi:10.1016/S0955-2219(00)00295-8

Longerich HP, Jackson SE, Gunther D (1996) Inter-laboratory note. Laser ablation inductively coupled plasma mass spectrometric transient signal data acquisition and analyte concentration calculation. J Anal Atom Spectrom 11:899–904. doi:10.1039/ja9961100899

Marfunin AS (1979) Physics of minerals and inorganic materials. Springer, New York

Ottinger F, Kroslakova I, Hametner K, Reusser E, Nesper R, Günther D (2005) Analytical evidence of amorphous microdomains within nitridosilicate and nitridoaluminosilicate single crystals. Anal Bioanal Chem 383:489–499. doi:10.1007/s00216-005-0057-y

Princivalle F, Della Giusta A, De Min A, Piccirillo EM (1999) Crystal chemistry and significance of cation ordering in Mg-Al rich spinels from high-grade hornfels (Predazzo-Monzoni, NE Italy). Mineral Mag 63:257–262

Rossman GR, Taran MN (2001) Spectroscopic standards for four- and fivefold-coordinated Fe^{2+} in oxygen-based minerals. Am Miner 86:896–903

Schmetzer K, Haxel C, Amthauer G (1989) Colour of natural spinels, gahnospinels and gahnites. Neues Jahrb Min Abhdl 160:159–180

Shigley JE, Stockton CM (1984) Cobalt-blue gem spinels. Gems Gem 20:34–41

Skogby H, Hålenius U (2003) An FTIR study of tetrahedrally coordinated ferrous iron in the spinel-hercynite solid solution. Am Miner 88:489–492

Taran MN, Langer K (2001) Electronic absorption spectra of Fe^{2+} ions in oxygen-based rock-forming minerals at temperatures between 297 and 600 K. Phys Chem Miner 28:199–210. doi:10.1007/s002690000148

Taran M, Koch-Müller M, Langer K (2005) Electronic absorption spectroscopy of natural (Fe^{2+}, Fe^{3+})-bearing spinels of spinel *s.s.*-hercynite and gahnite-hercynite solid solutions at different temperatures and high-pressures. Phys Chem Miner 32:175–188. doi:10.1007/s00269-005-0461-z

Taran MN, Koch-Müller M, Feenstra A (2009) Optical spectroscopic study of tetrahedrally coordinated Co^{2+} in natural spinel and staurolite at different temperatures and pressures. Am Miner 94:1647–1652. doi:10.2138/am.2009.3247